Unusual doping and temperature dependence of photoemission spectra from manganites

Prabuddha Sanyal[1,3], Subhra Sen Gupta[2,3], Nandan Pakhira[3,4],
H. R. Krishnamurthy[3,4], D. D. Sarma[3,4,5,6], and T. V. Ramakrishnan[3,4,7]
[1]*Harishchandra Research Institute, Allahabad 211019*
[2]*S.N. Bose National Center for Basic Sciences, Kolkata 700098*
[3]*Centre for Condensed Matter Theory (CCMT), Department of Physics, Indian Institute of Science, Bangalore 560012, India.*
[4]*Jawaharlal Nehru Centre for Advanced Scientific Research, Bangalore 560064, India.*
[5]*Solid State and Structural Chemistry Unit, Indian Institute of Science, Bangalore - 560012, India.*
[6] *Indian Association for Cultivation of Science, Kolkata 700032 and*
[7]*Department of Physics, Banaras Hindu University, Varanasi 221005, India.*

A recent, major, puzzle in the core-level photoemission spectra of doped manganites is the observation of a 1-2 eV wide shoulder with intensity varying with temperature T as the square of the magnetization over a T scale of order 200K, an order of magnitude less than electronic energies. This is addressed and resolved here, by extending a recently proposed two electron fluid $\ell - b$ model for these systems to include core-hole effects. The shoulder arises from a rapid redistribution of e_g electron density, as a function of T, between the highly localized(ℓ) and band-like (b) states. Furthermore, our theory leads to a correspondence between spectral changes due to increasing doping and decreasing T, as experimentally observed.

Doped rare earth manganites, $R_{1-x}A_x\mathrm{MnO_3}$ (R = rare earth ion; A = alkaline earth ion), show exotic properties such as colossal magneto-resistance [1] (CMR) close to a temperature (T) driven Ferro-metal (FM) to para-insulator (PI) or para-metal (PM) transition, an extraordinarily rich phase diagram with varying x, T and magnetic field (H), etc [2]. Particularly intriguing among their properties is the redistribution of spectral weight over an energy window of several eV in valence-band [3, 4] and Mn $2p$ core-level [5, 6] photoemission spectra (PES), as a function of x and of T. The changes in the spectral features with doping, incompatible with even an approximately *rigid-band* description, suggests qualitative and drastic modifications of the underlying electronic structure with small changes in x. Similarly, changes in T affect the spectra over energy ranges 100 times the thermal energy scale and cannot be understood in usual terms. Curiously, changes in spectra with increasing x or with decreasing T show striking similarities [4], suggesting a common mechanism. The effects have been attributed [3, 4] to the unusually strong electron-spin and electron-lattice couplings in these compounds, but no specific theory has been proposed till now.

Conventional core-level photoemission calculations, in terms of cluster models [7] or impurity models [8], can not account for a drastic renormalization of the underlying electronic structure with changing x or T. The only known mechanisms [9] that yield T dependent changes in PES are Fermi-edge decoherence (FED) effects due to thermal excitations and Debye-Waller type effects due to the scattering of electrons by phonons. They lead to changes only on energy scales of order T and the Debye temperature respectively ($\sim$ 10-100 meV), and not over several eV as observed. Cluster calculations [5] with *adjustable fitting parameters*, using an $\mathrm{MnO_6}$ octahedron coupled to a single level at the Fermi energy, reproduce the multiplet features of the observed spectra; but no x or T dependence, of the magnitude seen in the experiments, can arise unless the fitting parameters are *artificially* allowed to vary with x and T.

In this paper we adopt a radically different approach complementary to the above schemes, in that we focus on the x and T dependence, while neglecting details of multiplet structure. We employ the recently proposed *two-fluid 'ℓ-b' model* [10] in a dynamical mean-field theory (DMFT) [11] framework which successfully explains several hitherto poorly understood low energy properties of doped manganites. The active degrees of freedom in the manganites are the twofold degenerate e_g levels, the t_{2g} core-spins of Mn, and the Jahn-Teller (JT) optical phonon modes of the $\mathrm{MnO_6}$ octahedra. There are three strong on-site interactions, *viz.* the JT electron-phonon coupling which splits the two e_g levels by an energy $2E_{JT}$ ($\sim$ 0.5 - 1 eV), the ferromagnetic Hund's coupling J_H between the t_{2g} and e_g spins ($\sim$ 2 eV) and the e_g electron Coulomb repulsion U_{dd} ($\sim$ 5 - 7.5 eV)[12]; all larger than the e_g inter-site hopping ($t \sim$ 0.2-0.4 eV) [13] The 'ℓ-b' model[10] is an effective low energy Hamiltonian which implicitly captures the crucial effects of these interactions and the quantum dynamics of the JT phonons. It invokes two types of e_g electrons, one *polaronic* and *localized* (ℓ), and the other *band-like* and *mobile* (b), and is given by,

$$H_{\ell b} = (-E_{JT} - \mu) \sum_{i,\sigma} n_{\ell i\sigma} - \mu \sum_{i,\sigma} n_{bi\sigma}$$

$$+U_{dd} \sum_{i,\sigma} n_{\ell i\sigma} n_{bi\sigma} - t \sum_{<ij>,\sigma} (b^\dagger_{i,\sigma} b_{j,\sigma} + H.C.)$$

$$- J_H \sum_i (\vec{\sigma}_{\ell i} + \vec{\sigma}_{bi}) \cdot \vec{S}_i - J_F \sum_{<ij>} \vec{S}_i \cdot \vec{S}_j \qquad (1)$$

The *polaronically trapped* 'ℓ' species has site energy $-E_{JT}$, and an exponentially reduced hopping ($\sim 1\ meV$) which has been neglected, while the *non-polaronic* 'b' species (site energy 0) has undiminished hopping $t \sim$ 0.2-0.4 eV. J_F is a novel ferromagnetic *virtual double-exchange* (VDE) coupling ($\sim 2\ meV$) between the core spins, which arises naturally in this model [10]. The chemical potential, μ, imposes the doping determined filling constraint: $\sum_\sigma (\langle n_{\ell\sigma}\rangle + \langle n_{b\sigma}\rangle) = (1-x)$.

The 'ℓ-b' model is similar to the Falicov-Kimball model [14], and is exactly soluble in the DMFT [11] framework, with the t_{2g} core spins ($\vec{S}_i$) being approximated as classical vectors ($S\hat{\Omega}_i$) and J_F treated in the Curie-Weiss mean field approximation [10]. The resulting *self-consistent impurity model* [11], for a specific site, at any temperature T and in the limit of $J_H \to \infty$, depends parametrically on Ω_z (the z component of the unit vector representing the core-spin) at that site [10]. In order to calculate the Mn $2p$ core-level PES, we add to this a single 'core-hole' level (labeled 'c') of positive energy $\epsilon_c \approx 647.6eV$ at the impurity site [15]. The core hole has an attractive Coulomb interaction U_{pd} (= -6.5 eV) with both the 'ℓ' and the 'b' electrons. The resulting Hamiltonian reads :

$$H_{CL}(\Omega_z) = \sum_i (\epsilon_i - \mu) a_i^\dagger a_i + \sum_i V_i(\Omega_z)(a_i^\dagger b + b^\dagger a_i)$$

$$-(E_{JT} + \mu) n_\ell + \tilde{J}_F \langle m\rangle \Omega_z + (U_{dd} n_\ell - \mu) b^\dagger b$$

$$+ (\epsilon_c - \mu) n_c + U_{pd} n_c (b^\dagger b + n_\ell). \qquad (2)$$

Here, the $a_i^\dagger$ s create *bath* electrons, representing the 'b' electrons at the other sites of the lattice [11], with which the 'b' electrons of the chosen site hybridize; and which, for the purposes of this paper, we have approximated as having a discrete grid of energies $\{\epsilon_i\}$. The corresponding hybridization parameters $V_i(\Omega_z)$ are obtained from the $V(\epsilon;\Omega_z)$ determined self-consistently in the DMFT [10, 11]. $\tilde{J}_F = 2zJ_FS^2$ (z = coordination number) and $\langle m\rangle$ is the magnetization.

Both n_ℓ and n_c are conserved in H_{CL} (Eq. (2)). Hence, its eigenstates can be separately calculated in the 4 sectors: $(n_\ell, n_c) = (0,0)$, $(0,1)$, $(1,0)$ and $(1,1)$, labeled here as $(I0)$, $(F0)$ $(I1)$ and $(F1)$, respectively. One can therefore calculate a separate spectral function $A_{cc}(\omega; n_\ell, \Omega_z)$ in each n_ℓ sector, and for each Ω_z, as :

$$\sum_{m_0, m_1} \frac{e^{-\beta E_{m_0}}}{Z(\{m_0\})} | < m_1 | m_0 > |^2 \times \delta[E_{m_1} - E_{m_0} - \hbar\omega]$$

Here m_0, m_1 refer to the *many-body eigenstates* of H_{CL} in the $n_c = 0$ and $n_c = 1$ sectors respectively for the (n_ℓ, Ω_z) specified. The full core-hole spectrum is given by the weighted average

$$A_{cc}(\omega) = \sum_{n_\ell} \int_{-1}^{1} d\Omega_z W_{n_\ell}(\Omega_z) A_{cc}(\omega; n_\ell, \Omega_z)$$

where $W_0(\Omega_z)$ and $W_1(\Omega_z)$ are statistical weights obtained as $W_{n_\ell}(\Omega_z) = Z(n_l, n_c{=}0, \Omega_z)/Z$ using $Z(n_l, n_c, \Omega_z)$, the *constrained partition functions*, calculated for n_c=0 and for particular values of n_l and Ω_z; and Z is the total partition function.

The Boltzmann factors in the expression for $A_{cc}(\omega)$ give rise to the aforementioned FED effects in PES, which are very weak. However, special to our model, and hence to manganites, are two other, unconventional, sources of T and x dependence which are much larger: first, the statistical weights W_0 and W_1 are dependent on x and T; second, as we show below, the spectra for each (n_ℓ,Ω_z) themselves change with x and T, with redistribution of spectral weights over scales of eV, because the self consistent hybridization parameters $V_i(\Omega_z)$ are strongly x and T dependent [10]. Hence, for simplicity, we neglect the FED effects in this paper, by restricting m_0 above to just the ground state in the appropriate sector.

We have calculated the spectra using two different methods: (1) H_{CL} is single-particle like in each of the sectors (I0), (I1), (F0) and (F1), and can be *exactly diagonalized* for any Ω_z. The initial states, *i.e.* the *many-body ground state* (GS) for each n_ℓ, are obtained by filling up the single-particle levels in the $I0$ and $I1$ sectors up to the chemical potential [16]. The final ($n_c = 1$) many-body states are obtained by creating particle-hole (p-h) excitations with respect to the corresponding ground states, in the $F0$ and $F1$ sectors [16]. We find that the PES spectrum is dominated by the *single* p-h channel (spectral weight $> 95\%$) which is calculable [16] to very high accuracy even for a dense grid for the *bath* electrons. (2) More involved calculations including contributions from *all* p-h channels, but limited to using only 21 *bath* states, have been carried out using the Lanczos recursive algorithm [16]. In both cases, as is standard practice, the discrete spectra obtained have been broadened using a Gaussian broadening with $\sigma \sim 0.1\ eV$. The *single* and *all* p-h spectra are practically identical, and the small missing weight (3-5%) in the *single* p-h channel is visible only on close inspection. All the calculations reported in this paper are for model parameters appropriate for the LBMO thin-film samples of Tanaka *et al.* [6].

Our results of the doping variation of the PES, obtained at $T = 0$ in the fully spin-polarised FM phase ($\Omega_z = 1$), are shown in Fig. 1. Fig.s 1(a) and 1(b) show the spectra separately in the two n_l sectors and for both *single* and *all* p-h channels, for $x = 0.1$, 0.2, and 0.3. The *fully averaged spectrum* (Fig. 1(c)) thus has a *main peak* with *two shoulders*, one on each side , separated by about 6.5 eV ($\sim |U_{pd}|$) from a high energy *correla-*

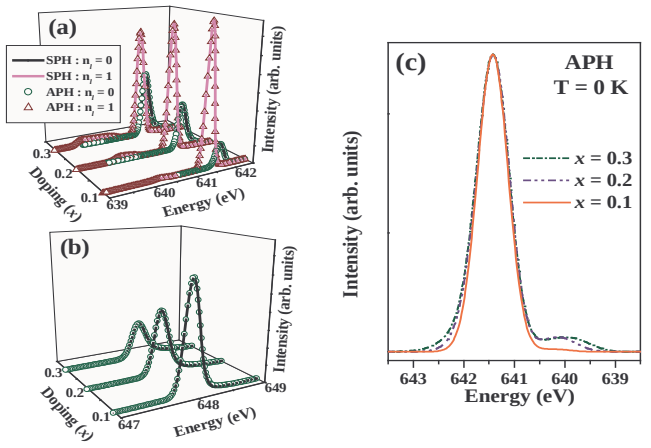

FIG. 1: (Color online) (a),(b) Calculated core-level PES spectra at $T = 0$, shown in two parts for clarity, in the *single p-h* (SPH) and *all p-h* (APH) channels, for the $n_l = 0$ and $n_l = 1$ sectors and for dopings 0.1, 0.2 and 0.3. (c) The fully averaged APH spectra for the three dopings (normalized to the main peak), showing only the main peak and the low energy shoulders.

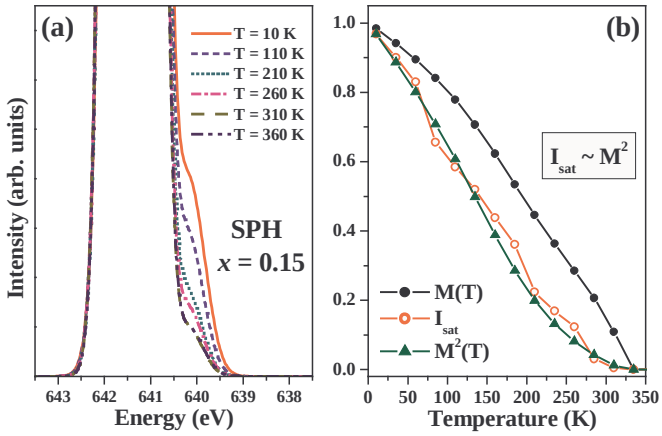

FIG. 2: (Color online) (a) Magnified view of the T dependence of the calculated spectra averaged over the two n_l sectors as well as the core spin angles, in the *single p-h* (SPH) channel for x=0.15. (b) The T dependence of the integrated shoulder intensity in the difference spectrum with respect to the paramagnetic spectrum, compared with $M^2(T)$, the square of the (DMFT derived) magnetization. $M(T)$ is also shown.

tion satellite (not shown in Fig. 1(c)) [17]. As seen in Fig. 1(c), with increasing x till about 0.3, the main peak intensity decreases, while those of the shoulders (and of the correlation satellite), increase substantially [17]. This is similar to what is seen in the core-level PES data in LSMO [5, 17]. In the data on LBMO [6] (where x is not varied), only the low energy shoulder is distinguishable. We believe that this is because LBMO has a lower x_c for the Ferro-Insulator (FI) to FM transition (0.05 as opposed to 0.16 in LSMO), and hence [10] a smaller (E_{JT}/D_0). In that case the small T dependent changes in the higher energy shoulder, separated only by $\sim E_{JT}$ from the main peak which is rather broad in the experiment, are harder to distinguish (see Fig. 2(a) where this effect is simulated using a broadening of 0.3 eV).

Fig. 2(a) shows a magnified view of T dependence of the fully averaged spectrum in the *single p-h* channel for x=0.15. Clearly, spectral changes as T *increases* are similar to the changes as x *decreases*, precisely as observed in LSMO [5]. In Fig. 2(b) we show the T dependence of the integrated shoulder intensity in the *difference spectrum* with respect to the paramagnetic spectrum, and find that it tracks $M^2(T)$, the square of the magnetization (as calculated using the DMFT). Such a correspondence has indeed been observed experimentally in LBMO [6], and is not reproducible by conventional rigid-band or cluster calculations.

All the major features of our calculated spectra can be understood from the *single p-h* channel contributions. Fig. 3 depicts the initial state and two important types of final states in each of the n_ℓ sectors in the metallic regime, with the bare bandwidth $D_0 = 1.3\ eV$, $E_{JT} = 0.29\ eV$. The 'b' band occupancy (n_b) is small and the chemical potential, pinned at $\mu \cong -E_{JT}$, lies close to the *effective* bottom edge, $-\tilde{D}$, of the 'b' band [18].

When $n_\ell = 0$ (Fig. 3(a)) the local 'b' level in the initial state $(n_c = 0)$ is at zero and hybridizes sparingly with the levels near the band edge, as the corresponding hybridization amplitudes are small. Thus the local 'b' character of the filled levels in the initial state is small. When $n_c = 1$, the local 'b' level is pulled down by an amount $|U_{pd}| = 6.5\ eV$, and becomes substantially occupied in the final GS. The local 'b' character of the occupied levels in the band is again very small. Hence in the $n_\ell = 0$ sector, the transitions involving *p-h* excitations with energies close to and above the spectral *edge* corresponding to the GS-to-GS transition ($\mu^- \rightarrow \mu^+$ in Fig. 3(a)), at an energy [19] $\sim (U_{pd} + \epsilon_c - 2\mu) \cong 641.68\ eV$, have low intensity. The dominant contribution comes from the transitions to final states where the local 'b' electron is excited to levels just above the chemical potential ($b \rightarrow \mu^+$ in Fig. 3(a)). The corresponding *edge* is at an energy [19] $\sim (-E_{JT} + \epsilon_c - 2\mu) \cong 647.89\ eV$ and leads to the correlation satellite in Fig. 1(a).

When $n_\ell = 1$ (Fig. 3(b)), the local 'b' level is pushed up, by an amount $U_{dd} = 5\ eV$, in the initial state $(n_c = 0)$. This further reduces the amount of 'b' mixing and hence the local 'b' character of the occupied levels in the initial state. When $n_c = 1$ (Fig. 3(b)), the 'b' level is at $(U_{dd} + U_{pd}) = -1.5\ eV$, much closer to the band edge than in the $n_\ell = 0$ sector. Nevertheless, the GS when $n_c = 1$ still has a substantial occupancy of the local 'b' level. Hence, the $\mu^- \rightarrow \mu^+$ transitions (Fig. 3(b)) again have a small intensity in the spectrum. The *edge* is now at an energy [19] $\sim (U_{dd} + 2U_{pd} + \epsilon_c - 2\mu) = 640.18\ eV$, $1.5\ eV$ below the *edge* in the $n_\ell = 0$ sector. Just

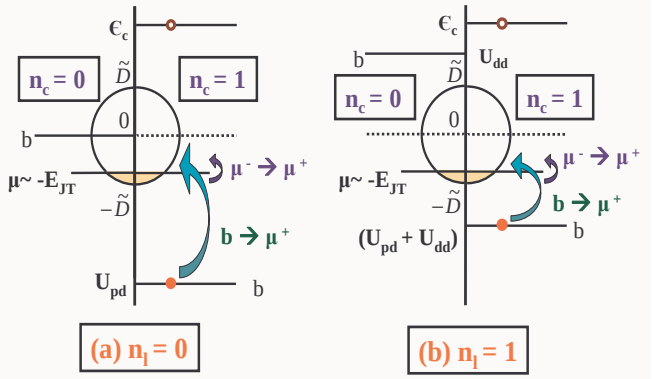

FIG. 3: (Color online) Schematic depiction of the GS configurations (with the occupied levels shown shaded) in the initial state ($n_c = 0$) and the ground and excited state configurations in the final state ($n_c = 1$) for the two sectors $n_l = 0$ (a) and $n_l = 1$ (b). Transitions to final states with the local 'b' level occupied have little intensity. The dominant transitions are to final states where the local 'b' electron has been transferred to just above the Fermi level.

as in the $n_\ell = 0$ sector, the main contribution to the spectrum comes from the $b \rightarrow \mu^+$ transitions (Fig. 3(b)), beyond the *edge* at an energy [19] $\sim (U_{pd} - E_{JT} + \epsilon_c - 2\mu) = 641.39\ eV$, hence below the GS-to-GS *edge* from the $n_\ell = 0$ sector. Associated with the *edge spectra* are edge singularities [20] and tails due to p-h excitations, which, when smoothed out, give rise to the shoulders with asymmetric [21] lineshapes.

As one increases x or decreases T, the 'b' bandwidth increases [18]. However, μ still remains close to $-E_{JT}$, so that the filling and the local 'b' character of the occupied band levels near μ increase in the initial state. Hence, one gets a steady transfer of spectral weight from the features where the local 'b' level is unoccupied in the final state, to those where it is occupied in the final state, as seen in the bare or un-averaged spectra (Fig. 1(a)). The spectra shown in Fig. 1(b) are averaged over the contributions from the two n_ℓ sectors (and additionally over Ω_z for Figs. 2(a) and 2(b)), with statistical weights which are themselves functions of x and T. The net effect is that the two shoulders on the two sides of the main peak, arising from smoothed out edge spectra as shown above, increase in intensity with increasing x or decreasing T, in agreement with experiments.

In conclusion, we have presented Mn $2p$ core-level PES calculations by extending a new model for manganites [10] that takes into account the simultaneous presence of strong *electron-lattice*, *spin-spin* and *charge-charge* interactions. Our results reproduce, for the first time, the unusual redistribution of spectral weight over several eV upon varying x and T, and a correspondence between the effect of increasing x and decreasing T, as experimentally observed [5, 6].

We would like to thank the JNCASR (NP,SSG) and the DST (HRK,PS,DDS) for financial support.

[1] S. Jin *et al.*, Science **264**, 413 (1994); K. Chahara, T. Ohno, M. Kasai, Y. Kozono, Appl. Phys. Lett. **63**, 1990 (1993).
[2] See *e.g.* M. B. Salamon, M. Jaime, Rev. Mod. Phys. **73**, 583 (2001)
[3] D. D. Sarma *et al.*, Phys. Rev. B **53**, 6873 (1996).
[4] T. Saitoh *et al.*, Phys. Rev. B **56**, 8836 (1997).
[5] K. Horiba *et al.*, Phys. Rev. Lett. **93**, 236401 (2004).
[6] Hidekazu Tanaka *et al.*, Phys. Rev. B **73**, 094403 (2006).
[7] S.R. Barman, A. Chainani and D. D. Sarma, Phys. Rev. B **49**, 8475 (1994).
[8] O. Gunnarson, K. Schonhammer, D. D. Sarma, F. U. Hillebrecht and M. Campagna, Phys. Rev. B **32**, R5499 (1985); D. D. Sarma and A. Taraphder, Phys. Rev. B **39**, 11570 (1989).
[9] K. Ohtaka and Y. Tanabe, Rev. Mod. Phys. **62**, 929 (1990), and references therein.
[10] T.V. Ramakrishnan, H.R. Krishnamurthy, S.R. Hassan and G.Venketeswara Pai, Phys. Rev. Lett. **92**, 157203 (2004) and Condmatt-0308396; G.V. Pai, S.R. Hassan, H.R. Krishnamurthy and T.V. Ramakrishnan, EuroPhys. Lett. **64**, 696 (2003); S.R. Hassan, Ph.D. Thesis, Indian Institute of Science (2003).
[11] A. Georges, G. Kotliar, W. Krauth, and M. J. Rozenberg, Rev. Mod. Phys. **68**, 13 (1996).
[12] A.E. Bocquet *et al.*, Phys. Rev. B **46**, 3771 (1992).
[13] D. D. Sarma *et al.*, Phys. Rev. Lett. **75**, 1126 (1995); S. Satpathy, Z. S. Popovic, and F. R. Vukajlovic, Phys. Rev. Lett. **76**, 960 (1996); P. Mahadevan, N. Shanthi, and D. D. Sarma Phys. Rev. B **54**, 11199 (1996).
[14] J. K. Freericks and V. Zlatic, Rev. Mod. Phys. **75**, 1333 (2003).
[15] H. D. Kim, H. J. Noh, K. H. Kim and S. J. Oh, Phys. Rev. Lett. **93**, 126404 (2004).
[16] Our initial and final many-body states are thus *direct products of the occupied single particle states*, with first-quantized wavefunctions that correspond to Slater determinants. In the spectral calculations, we compute matrix elements involving the overlap of such determinants. *For a given discretization of the bath, our all-particle-hole calculations of the spectra are model-exact, and satisfy all the exact sum rules.*
[17] In reality, we expect these features to ride on a broad, largely T, x independent, background [5, 6] arising from multiplet and charge-transfer interactions with the ligands that are neglected in the present calculation. We expect that the correlation satellite is hardly observable [5] for the same reason, its weight getting transferred to the shoulders, raising their intensity to the observed levels, as confirmed by preliminary model calculations [22]. Accordingly, for comparison with data [6] we compare *difference spectra*, as in Fig. 2(b), where this background gets subtracted out.
[18] As discussed in detail in [10], the hopping of the 'b' electrons is inhibited by an annealed random medium of repulsive sites occupied by the 'ℓ' polarons. At nonzero T, the t_{2g} spins (to which the 'ℓ' and 'b' spins are enslaved by the large J_H) get thermally disordered. In either case, the

resulting scattering leads to an effective bandwidth $2\tilde{D}$ much smaller than the bare bandwidth $2D_0$, but which increases substantially as x increases or as T decreases.

[19] The energies quoted in the text for the *edges* are approximate as they do not include the contributions from the hybridization terms.

[20] Using a *logarithmic discretization of the band*, we have calculated CL-PES spectra that accurately capture the edge *singularities* as well as reproduce the results presented here [22]. The exponents for both the n_ℓ=0 (exponent$\sim$ -0.823) and n_ℓ=1 (exponent$\sim$ -0.236) sectors agree with the theory of Noziers and DeDominicis based on phase shift analysis [9]. However, with current core-level PES resolutions these are unobservable experimentally. The linear discretization calculations capture the smoothed out, higher energy features we focus on in our paper with less computational effort [22].

[21] S. Doniach and M. Sunjić, J. Phys. C **3**, 285 (1970).

[22] The details will be published elsewhere. See also Prabuddha Sanyal, Ph.D. Thesis (Indian Institute of Science, 2006) (to be submitted); Subhra Sen Gupta, Ph.D. Thesis (Indian Institute of Science, 2006) (to be submitted).